Journal of
Experimental
Botany
www.jxb.oxfordjournals.org

RESEARCH PAPER

Genome-wide analysis of the UDP-glucose dehydrogenase gene family in *Arabidopsis*, a key enzyme for matrix polysaccharides in cell walls

Michaela Klinghammer[1] and Raimund Tenhaken[2,*]

[1] *University of Frankfurt, Plant Molecular Biology, Biocenter, D-60439 Frankfurt, Germany*

[2] *University of Salzburg, Plant Physiology, Hellbrunnerstr. 34, A-5020 Salzburg, Austria*

Abstract

Arabidopsis **cell walls contain large amounts of pectins and hemicelluloses, which are predominantly synthesized via the common precursor UDP-glucuronic acid. The major enzyme for the formation of this nucleotide-sugar is UDP-glucose dehydrogenase, catalysing the irreversible oxidation of UDP-glucose into UDP-glucuronic acid. Four functional gene family members and one pseudogene are present in the** ***Arabidopsis*** **genome, and they show distinct tissue-specific expression patterns during plant development. The analyses of reporter gene lines indicate gene expression of UDP-glucose dehydrogenases in growing tissues. The biochemical characterization of the different isoforms shows equal affinities for the cofactor NAD^+ ($\sim$40 μM) but variable affinities for the substrate UDP-glucose (120–335 μM) and different catalytic constants, suggesting a regulatory role for the different isoforms in carbon partitioning between cell wall formation and sucrose synthesis as the second major UDP-glucose-consuming pathway. UDP-glucose dehydrogenase is feedback inhibited by UDP-xylose. The relatively (compared with a soybean UDP-glucose dehydrogenase) low affinity of the enzymes for the substrate UDP-glucose is paralleled by the weak inhibition of the enzymes by UDP-xylose. The four** ***Arabidopsis*** **UDP-glucose dehydrogenase isoforms oxidize only UDP-glucose as a substrate. Nucleotide-sugars, which are converted by similar enzymes in bacteria, are not accepted as substrates for the** ***Arabidopsis*** **enzymes.**

Key words: Cell wall precursor, gene expression, hemicellulose, nucleotide-sugar, UDP-glucose dehydrogenase.

Introduction

Plant cells are surrounded by a rigid but often flexible cell wall to counterbalance the high osmotic pressure inside the cells. Therefore, plant growth requires extensive synthesis of cell wall material during development. The principal composition of *Arabidopsis* cell walls, analysed from leaves of 4–5-week-old plants, was determined previously (Zablackis *et al.*, 1995). This study indicates a high amount of pectic polymers and hemicelluloses, together forming the matrix polysaccharides, in which cellulose fibrils are embedded along with cell wall structural proteins. Matrix polysaccharides are synthesized in the Golgi apparatus by polymer synthases, which require nucleotide-sugars as glycosyl donors. Excellent reviews of the complex nucleotide-sugar interconversion pathways have been published recently (Gibeaut, 2000; Reiter and Vanzin, 2001; Seifert, 2004). Based on the study by Zablackis *et al.* (1995), one can calculate that $\sim$50% of the cell wall biomass is derived from the precursor UDP-glucuronic acid (UDP-GlcA). This nucleotide-sugar is the direct precursor of UDP-galacturonic acid after epimerization (Mølhøj *et al.*, 2004; Usadel *et al.*, 2004), UDP-xylose and UDP-apiose after decarboxylation (Kobayashi *et al.*, 2002), and UDP-arabinose derived from UDP-xylose by an epimerase (Burget *et al.*, 2003). Plants have evolved two independent pathways for the synthesis of UDP-GlcA; this fact underlines the importance of this nucleotide-sugar for plant growth. One pathway involves the direct oxidation of UDP-glucose (UDP-Glc) into UDP-GlcA by the enzyme UDP-glucose dehydrogenase (UDP-α-D-glucose:NAD^+ oxidoreductase; EC 1.1.1.22; UGD) (Tenhaken and Thulke, 1996). Alternatively, UDP-GlcA can be formed in a more complex reaction via ring

* To whom correspondence should be addressed. E-mail: raimund.tenhaken@sbg.ac.at

cleavage of *myo*-inositol into glucuronic acid, followed by subsequent activation of the sugar to UDP-GlcA (Loewus *et al.*, 1962; Seitz *et al.*, 2000; Kanter *et al.*, 2005). Because of the unique entry enzyme of the pathway, *myo*-inositol oxygenase (MIOX), this route is often referred to as the MIOX pathway for UDP-GlcA formation.

The UGD enzyme uses UDP-Glc, available from photosynthesis assimilates, as a substrate. The major competing alternative pathway for the consumption of UDP-Glc is the synthesis of sucrose-6-phosphate by the enzyme sucrose-6-phosphate synthase (SPS), which provides the precursor for the major phloem metabolite sucrose (Winter and Huber. 2000). In addition, UDP-Glc may also be used directly as a glycosyl donor for cellulose synthase or for the formation of callose at the plasma membrane.

UGD oxidizes the C6 carbon of glucose from an alcohol to a carbonic group in two subsequent oxidation reactions with no release of intermediates (Ge *et al.*, 2004). The overall reaction is energetically irreversible, with the consequence that UDP-GlcA can be used exclusively for the synthesis of cell wall matrix polysaccharides, glucuronylation of secondary compounds, and post-translational modification of glycoproteins. The separation of the nucleotide-sugars into a pool of mostly cell wall-specific precursors (UDP-GlcA, UDP-GalA, UDP-Ara, UDP-Xyl, and UDP-apiose) and a pool used for the synthesis of storage compounds (sucrose) and cell walls (UDP-Glc and UDP-Gal) raises the question of which UDP-sugar(s) feed into the cell wall precursor pool (Seifert, 2004). Whereas UDP-Glc is undoubtedly the major substrate for UGDs, it is discussed controversially whether UDP-galactose could be a direct precursor of UDP-galacturonic acid for pectic polymers (Stewart and Copeland, 1998).

The first gene for a eukaryotic *UGD* was cloned from soybean (Tenhaken and Thulke, 1996). From measuring the enzymatic activity and analysing public DNA databases, it is evident that *UGD* genes are present in almost all organisms, with the exception of a few with a secondarily reduced genome like the yeast *Saccharomyes cerevisiae*. Often several isoforms of UGD are present in plants, a finding which has only been studied in maize so far (Karkonen *et al.*, 2005). Most papers on plant UGDs have either ignored the existence of isoforms or performed a combined analysis of several isoforms simultaneously. Here the analysis of the *UGD* gene family of *Arabidopsis* is reported to give a comprehensive overview of the gene expression of different isoforms and their biochemical properties.

Materials and methods

Bioinformatics

To identify all *UGD*-like genes from *Arabidopsis* the public databases in GenBank were searched. All expressed sequence tag (EST) sequences with high similarity to UGD could be assigned to one of the four *UGD* genes present in the sequenced *Arabidopsis* genome.

A fifth *UGD* gene with a weaker similarity was detected at the top of chromosome 3. A detailed analysis suggested a partial sequence of an additional *UGD* gene (*UGD5*). To rule out any assembling error in the genome project, the genomic situation for this region was verified by PCR. The primers GCCGGAACAG-GATTAGGCTT and CTAGAGGAGACGCCTGTAAC from the flanking neighbouring genes amplified a product of the predicted size (1381 bp) according to the data in the genome project.

Reporter gene analysis

The promotor sequences of *UGD1*, *2*, *3*, and *4* were amplified by PCR using the primer combinations given in Table 1. Genomic DNA from *Arabidopsis thaliana* was used as template. PCR products were cloned in front of the *uidA* gene of vector pBI101 (Clontech MountainView, CA, USA) (*UGD1*, *2*, and *3*) or pGreen (http://www.pgreen.ac.uk) (*UGD4*) via the relevant restriction cleavage sites.

Cloning products were verified by DNA sequencing (Seqlab, Göttingen, Germany) and plasmids were transferred into *Agrobacterium tumefaciens* GV 3101. Subsequently, *A. thaliana* Col-0 plants were transformed by the floral dip method developed by Clough and Bent (1998). Several independent transformants were stained for β-glucuronidase (GUS) activity and a typical line was chosen for detailed analysis.

For reporter gene analysis, seedlings were grown sterile on 0.5× MS medium (#M0245, Duchefa Biochemie, Haarlem, The Netherlands), pH 5.7 (KOH) with 0.5% (w/v) sucrose and 0.25% (w/v) Phytagel™ (Sigma-Aldrich, Munich, Germany) or on soil in growth chambers (23 °C, 50% relative humidity). Plants were cultured either with an 8 h light period (fluorescent bulbs ∼100 μE m^{-2} s^{-1}) or in the dark. Seedlings of different developmental stages and distinct plant tissues were collected and stained with X-Gluc for GUS activity for 5 min–16 h, using the protocol of Jefferson (1987). Plants were photographed with a Leica stereo microscope (Leica MZFL III, Solms, Germany), equipped with a digital camera (Canon PowerShot S40). Pictures were assembled in Adobe PhotoshopCS 8.0.1.

Total RNA isolation and real-time PCR

For total RNA isolation, seedlings were grown sterile on MS plates in growth chambers for 6 d with 8 h light periods or in the dark as described above. About 100 mg of plant material (light-grown seedlings, etiolated seedlings, roots, and cotyledons/hypocotyl of seedlings) were collected, frozen in liquid nitrogen, and homogenized by a ball mill (Retsch MM200, 3×30 s, frequency 30 Hz). Total RNA was isolated by the acid phenol/guanidinium thiocyanate method (Chomczynski and Sacchi, 1987). First-strand cDNA was synthesized by using a RevertAid™ M-MuLV Reverse Transcriptase Kit (Fermentas GmbH), according to the supplier's protocol, and 3 μg of total RNA.

Real-time PCR was performed using 1 μl of a 1/20 (v/v) dilution of first-strand cDNA reaction, 1× reaction buffer [10 mM TRIS-HCl pH 8.5, 50 mM KCl, 0.15% Triton X-100, 2.5 mM MgCl₂ (Karsai *et al.*, 2002)], 200 μM dNTPs, 200 nM of each primer, SYBR green (Roche, Mannheim, Germany) diluted to a 1:200 000 concentration, and 1.5 U of *Taq* (total reaction volume 30 μl) using a Stratagene Mx3000P QPCR system (Statagene, La Jolla, CA, USA). For primer oligonucleotide sequences, see Table 1. PCR was conducted using the following amplification conditions: 94 °C for 3 min, 40× [94 °C for 30 s, 65 °C (*UGD1* and *3*), 57 °C (*UGD2*), or 58 °C (*UGD4*) for 45 s, 72 °C for 1 min], 95 °C for 1 min, 65 °C for 30 s. Each primer pair amplified a single product, as indicated by the melting curve of the amplicons. The resulting C_T

Table 1. *Primer sequences used for constructs and mRNA amplification*

Gene	Primer	Application
UGD1	5′-GCCTCGAGATTAGACGGTTTTAAATACGC 5′-TTGGATCCTTCTGATTTTCAAAACGTCTCCTGTT-3′	UGD1 promotor cloning
	5′-GTGATGGCTCTTAAGTGTCCTG-3′ 5′-ATGGTACCGTTGGCACCTTCATGCCAC-3′	Cloning expression vector pQEUGD1
	5′-ATGGATCCAATGGTGAAGATATGCTGCATAG-3′ 5′-GTCTCGAGCAATGCCACAGCAGGCATA-3′	Cloning expression vector pET21aUGD1
	5′-TGAAGATATGCTGCATAGGAGCTGGTTAT-3′ 5′-ATCCTTGAGCCATGAATCAAGCGGTTTAC-3′	Real-time PCR
UGD2	HindIII/EcoRV fragment (18 000 bp) from a genomic library	UGD2 promotor cloning
	5′-GCACTTAAGTGTCCAGACGTTGAAGTAG-3′ 5′-ACGGTACCTGTCGAATACAAGTCCTCTT-3′	Cloning expression vector pQEUGD2
	5′-AACACACCGACTAAGACTAGAG-3′ 5′-TAGCTTTTGCAGATTCATAATGTTTC-3′	Real-time PCR
UGD3	5′-ACGTAAGCTTACTATGAATGGACATTGACGCACAG 5′-ACGTGGATCCTTGTAAACTGAATCACCTCCTGTG	UGD3 promotor cloning
	5′-GCTCTTAAGTGTCCATCTGTTGAAGTAG-3′ 5′-ACGGTACCACCCAAGGTACATAATTACC-3′	Cloning expression vector pQEUGD3
	5′-GTCCAACCATGGCTGTCATTGCTCTAAAG-3′ 5′-GGTCCAATGGCTTACCAATGGAGTAAACA-3′	Real-time PCR
UGD4	5′-ACCTCGAGACGATATTGCCCATGTCT-3′ 5′-ATCCCGGGTCCAGCTCCAATACAACAG-3′	UGD4 promotor cloning
	5′-GCACTTAAGTGTCCAGATATTGAAGTGGC-3′ 5′-GTTTTCCCAGTCACGACGTTTGTA-3′	Cloning expression vector pQEUGD4
	5′-GGGTCAAGTGGCTTACCAAT-3′ 5′-GCACTTAAGTGTCCAGATATTGAAGTGGC-3′	Real-time PCR

values were normalized to the average of the Ct values of the transcript of the housekeeping gene ubiquitin-5 (At3g62250) (Karsai *et al.*, 2002) amplified under the following conditions: 94 °C for 3 min, 40× (94 °C for 15 s, 56 °C for 20 s, 72 °C for 20 s), 95 °C for 1 min, 65 °C for 30 s.

Expression vector constructs

For cloning into expressions vectors, the open reading frame (ORF) of each *UGD* was amplified by PCR (Phusion High-Fidelity DNA Polymerase Kit, New England Biolabs) using the primer combinations listed in Table 1 and full-length EST clones as templates: *UGD1*, M77J01; *UGD2*, AV43959; *UGD3*, 43C9T7; and *UGD4*, 105N9T7 (Arabidopsis Stock Center). The PCR products were cloned into pQE31 (Qiagen, Hilden, Germany; *UGD2–4*) or into pET21a (*UGD1*) (Novagen, Darmstadt, Germany) via the relevant restriction cleavage sites. Each construct was confirmed by DNA sequencing (Seqlab, Göttingen, Germany).

The expression vector constructs were co-transformed with pGroESL (Amrein *et al.*, 1995) into the *Escherichia coli* expression strain Origami™ (Novagen, Darmstadt, Germany).

Protein expression and purification

The *E. coli* expression strains were routinely grown in LB medium containing 100 μg ml^{-1} ampicillin, 34 μg ml^{-1} chloramphenicol, 20 μg ml^{-1} tetracyclin and 50 μg ml^{-1} kanamycin at 37 °C overnight, inoculated at 1/100 dilution in LB medium (antibiotics as above), and cultured to an OD$_{600}$ of ~0.4 under vigorous shaking. After cooling the cultures for 15 min at room temperature, protein expression was induced by addition of 500 μM isopropyl-β-D-thiogalactopyranoside (IPTG). The cultures were grown at 23 °C for a further 20 h.

After cooling the cultures by shaking for 15 min on ice, cells were harvested by centrifugation (10 min at 4500 *g* and 4 °C) and frozen in liquid nitrogen after discarding the supernatant. Subsequently, cells were thawed in 10 ml g^{-1} FW chilled disruption buffer [50 mM sodium phosphate, 10 mM TRIS-HCl pH 8.0, 10% (v/v) glycerol, 2 mM MgCl$_2$, 2 mM 2-mercaptoethanol, 1 mM NAD$^+$, 0.2 mM phenylmethylsulphonyl fluoride (PMSF, disolved in isopropanol)] by vigorous vortexing. Lysozyme at 200 μg ml^{-1} and 1% (v/v) Nonidet P-40 were added and shaken slowly on ice for 45 min to disrupt bacterial cells gently. Bacterial debris was removed by centrifugation for 10 min at 14 500 *g* and 4 °C. The supernatant was transfered into a new tube; 2.4 U ml^{-1} benzonase nuclease HC (Novagen, Darmstadt, Germany) was added and incubated for 15 min by shaking slowly on ice. The clear supernatant was applied to a Ni-NTA-agarose column (Qiagen, Hilden, Germany) equilibrated with NTA-1 buffer [50 mM sodium phosphate, 10 mM TRIS-HCl pH 8.0, 250 mM NaCl, 10% (v/v) glycerol, 0.5 mM NAD$^+$], after addition of 250 mM NaCl. The column was washed with 5 vols of NTA-1 buffer and 5 vols of NTA-2 buffer (NTA-1 buffer with 20 mM imidazole) to remove all weakly bound proteins. UGD proteins were eluted by addition of 2.5 vols of NTA-3 buffer (NTA-1 buffer with 250 mM imidazole). The enzymes were immediately transferred into storage buffer [20 mM TRIS-HCl pH 8.7, 50 mM KCl, 10% (v/v) glycerol, 0.5 mM NAD$^+$] by gel filtration on a PD10 column (Amersham Bioscience, Freiburg, Germany). The enzymes could be stored at –80 °C (>6 months) after being frozen in liquid nitrogen without any reduction in activity. UGD protein purification was verified by SDS–PAGE.

The yeast strain Toy4, expressing a His-tagged version of *Arabidopsis* UGD1, was a kind gift of Dr Y Jigami. UGD1 was expressed and purified from a yeast extract according to Oka and Jigami (2006).

Enzyme assays and kinetic analysis

The enzyme activity of UGD was determined photometrically at 340 nm (Beckmann photometer DU640) by the increase of NADH. The assays were performed for 1–10 min at room temperature in assay buffer [40 mM TRIS-HCl pH 8.7, 0.8 mM EDTA, 16% (v/v) glycerol, 0.8 mM NaN$_3$]. For the determination of kinetic parameters, (i) saturated concentrations of NAD$^+$ (500 μM) and various concentrations of UDP-glucose (0.01–1.5 mM) were used; or (ii) various NAD$^+$ concentrations (0.01–1.5 mM) and a constant

UDP-glucose concentration (2 mM) were used. The amount of the UGD added was based on enzymatic activity and was set to 0.03 OD$_{340}$ units change per minute. The final reaction volumn was set to 1 ml. Triplicate values were obtained for each measurement, and data were plotted with Microcal Origin 6.0G Professional. The K_m values were calculated from the hyperbolic curve using the least-square algorithm of the Origin-software.

Product analysis

The substrates and products of UGD enzyme assays were analysed by high-performance liquid chromatography (HPLC; Dionex U3000 system) using ion-pair chromatography on an RP18-column (Prontosil 120 C18 AQ-Plus 150×3 mm). Separation was performed in buffer A (25 mM tetraethylammonium acetate; pH 6) for 8 min, followed by a linear gradient to 25% buffer B (buffer A plus 20% acetonitrile) for 10 min using a flow rate of 0.5 ml min^{-1}. UV spectra were recorded from 240 nm to 300 nm and plotted for the wavelength 260 nm. The reference compounds UDP-Glc was from MP-Biomedical; UDP-Gal, UDP-glucuronic acid, and UMP were purchased from Sigma.

Results

Identification of the UGD genes in Arabidopsis

In *Arabidopsis*, the *UGD* gene family is represented by four transcribed members (*UGD1–4*) and one pseudogene (UGD1, At1g26570; UGD2, AT3g29360; UGD3, At5g15490; and UGD4, At5g39320). The *Arabidopsis* UGD described earlier (Seitz *et al.* 2000) is termed UGD2 herein. The four *UGD*s encode very similar proteins of 480–481 amino acids. The difference (including conserved exchanges) in the amino acid sequence is <10% between the four iso-forms (Fig. 1). The schematic structure of the (pre)-mRNA
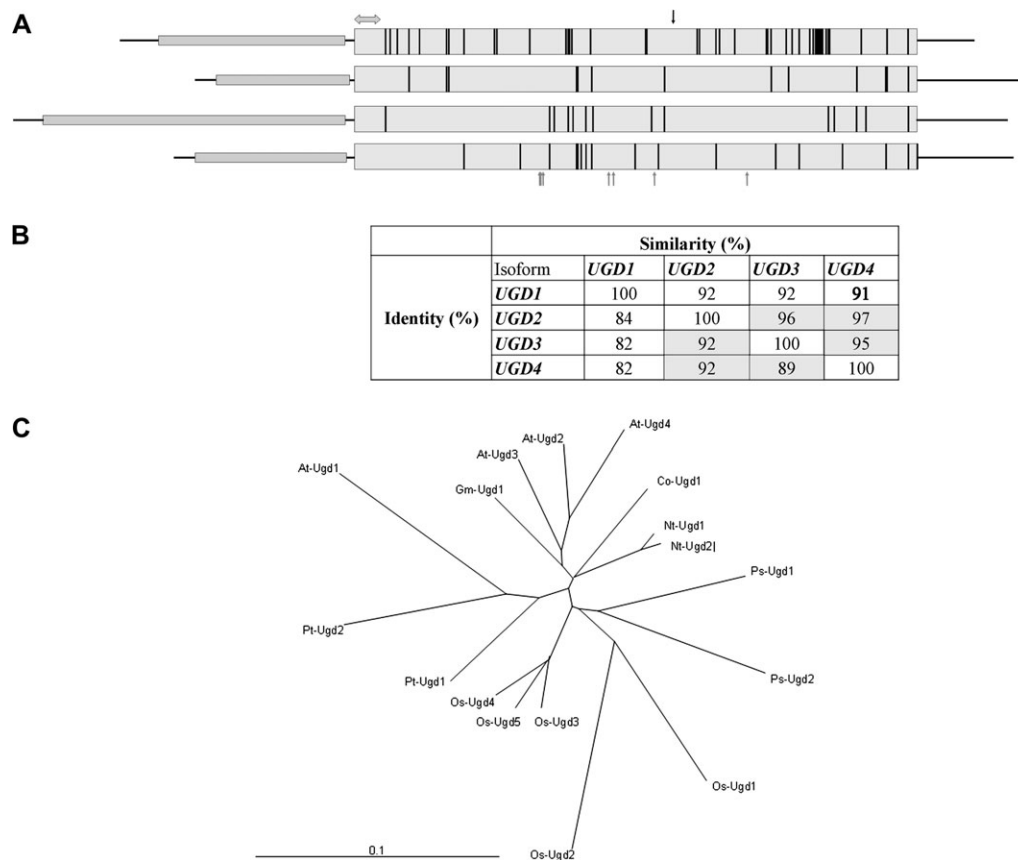
Fig. 1. Schematic structure of primary RNA transcript protein sequences for *UGD* genes. (A) All four *UGD* genes contain a single intron in the 5' untranslated region, represented by small boxes. The larger boxes represent the ORFs of *UGD1–4*. Each single amino acid change from the consensus sequence is represented by a black line in the ORF. The double-headed arrow above the sequences shows the NAD$^+$-binding site. The downward pointing arrows above the sequences indicate the cysteine residue essential for catalyis in all UGDs. The upward pointing arrows below the bars indicate the position of all amino acids involved in glucose binding of UDP-Glc, which are positionally conserved between the UGDs from *Arabidopsis* and the UGD from *Streptococcus pyogenes*, for which a crystal structure is available (Campbell *et al.*, 2000). (B) The table shows the percentage amino acid identity (left lower triangle) or similarity (right upper triangle) between the four different UGD isoforms. The sequences of UGD2, 3, and 4 are highly similar, but UGD1 differs significantly from the other sequences. (C) Aligment of some plant UGD sequences with ClustalX. The UGD1 from *Arabidopsis* clusters together with the two poplar sequences, distinct from the other *Arabidopsis* branch [At-UGD1-4 (this paper); Co-UGD1, *Cinnamomum osmophleum* gil40317278; *Glycine max* Gm-UGD1, gil6136119; *Nicotiana tabaccum* Nt-UGD1, gil48093457; *Nicotiana tabaccum* Nt-UGD2, gil48093459; Ps-UGD1, *Pinus taeda* Unigene Pta.24139; Ps-UGD2, *Pinus taeda* Unigene Pta.8150; *Oryza sativa* Os-UGD1, Os03g31210; *Oryza sativa* Os-UGD2, Os03g40720; *Oryza sativa* Os-UGD3, Os03g55070; *Oryza sativa* Os-UGD4, Os12g25690; *Oryza sativa* Os-UGD5, Os12g25700; Pt-UGD1, *Populus trichocarpa* eugene3.00041110; *Populus trichocarpa* Pt-UGD2, eugene3.00101501].

is shown in Fig. 1. All of the four *UGD*s contain a single intron of variable length in the 5' untranslated region whereas the full ORF is not disrupted by further introns. The amino acid sequence variations between the four isoforms are not uniformly distributed along the whole sequence and between all isoforms. Clustering of amino acid exchanges occurs between different pairs of UGDs, indicating that a simple recent gene duplication event does not account for the four UGD isoforms in *Arabidopsis*.

Based on the crystal structure of a UGD from *Streptococcus pyogenes* (Campbell *et al*., 2000), all of the amino acid residues involved in substrate binding and catalysis are absolutely conserved between the enzyme from bacteria and plants. The residues involved in binding the UDP-glucose are highlighted schematically in Fig. 1. Several plant UGD sequences were aligned using ClustalX to generate a bootstrapped Neighbor–Joining tree (Fig. 1C). The tree indicates a close proximity of *Arabidopsis* UGD2, 3, and 4, which cluster together with a UGD from soybean, but puts *Arabidopsis* UGD1 on a different branch. UGDs from rice cluster into groups of the same branch. Similarly, the two sequences from tobacco, *Pinus tadea*, and *Populus* each group together, suggesting gene duplication events after speciation. Further UGD sequences of EST libraries were not included because in many cases the algorithm for generating UNIGENE sequences in GenBank puts sequences from different isoforms into a single data set (e.g. tested for soybean; data not shown).

The pseudogene is lacking about two-thirds of the coding sequence including the NAD^+-binding site, which is essential for catalytic activity. The chromosomal location at the very beginning of chromosome 3 suggests a segmental gene duplication during evolution, as indicated by the doubling of 37 recognized ORFs (At3g01010–At3g02020) matching a highly similar region on chromosome 5 (At5g15510–At5g14060).

Expression pattern of UGD *genes in* Arabidopsis

Promoter::GUS fusion constructs were used in stably transformed *Arabidopsis* plants to compare gene expression patterns of *UGD1–4*. The homozygous transgenic lines were analysed for each construct and a typical line was selected for a detailed analysis of the reporter gene activity. The pattern of the most abundantly active reporter *UGD2::GUS* is shown in Fig. 2 (compare also Fig. 4). *UGD2::GUS* activity is seen first during the germination process in 1-d-old seedlings, when the radicle breaks through the seed coat (Fig. 2a). In seedlings up to 5 d old, the activity of *UGD2::GUS* is restricted to the primary root (Fig. 2b). In particular, *UGD2::GUS* activity can be detected in roots tips, in young root hairs, and in the calyptra. In further growth phases, cotyledons show an even but low activity of the *UGD2::GUS* reporter gene, which is still highest in the roots (Fig. 2c, d). This pattern remains similar for the vegetative phase of the life cycle (Fig. 2e). Growth of seedlings in the dark leads to etiolated
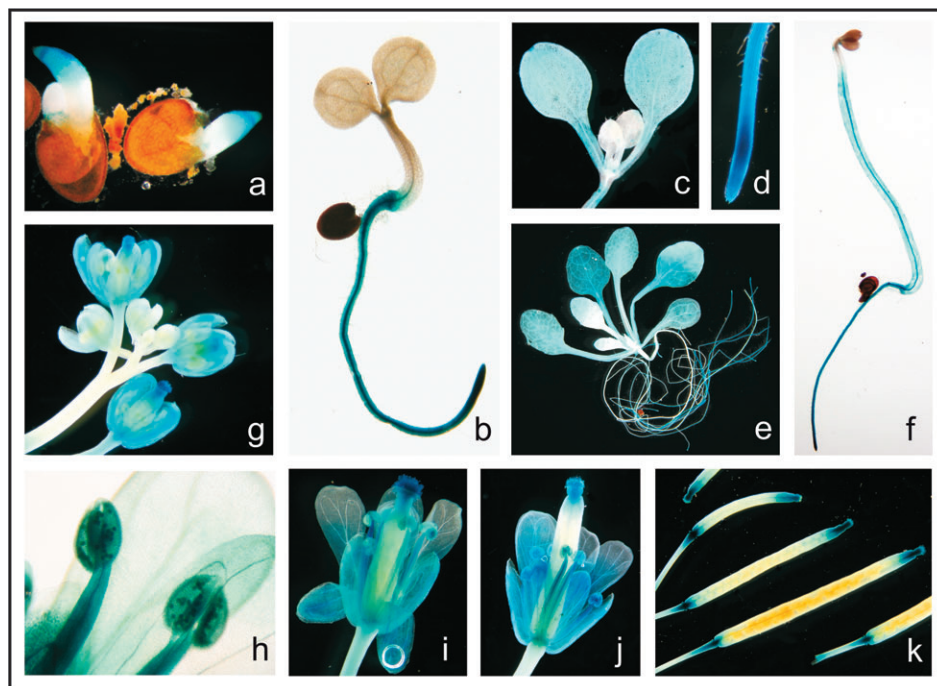
Fig. 2. Reporter gene expression of *UGD2::GUS* in transgenic *Arabidopsis thaliana* plants. Different tissues and development stages are shown. Seedlings were grown in light (a–e, g–k) or dark conditions (f): (a) 1-d-old seedlings; (b) 3-d-old seedling; (c) cotyledons of a 7-d-old seedling; (d) root tip; (e) 2-week-old *Arabidopsis* plant; (f) etiolated 4-d-old seedling; (g) buds and young flowers; (h) pollen sacs containing mature pollen; (i) older flower; (j) pollinated flower with developing silique; (k) different silique stages.

and elongated hypocotyls showing a strong *UGD2::GUS* activity in the hypocotyl (Fig. 2f). This reporter gene activity is absent in light-grown seedlings (Fig. 2b). In roots of etiolated seedlings a similar expression pattern to that of light-grown seedlings can be detected. During germination and the vegetative phase of the life cycle, a close correlation between growth, requiring UDP sugars for the synthesis of matrix polysaccharides, and the activity of the UGD2::GUS reporter is generally seen. The more complex pattern of *UGD2::GUS* activity in flowers and siliques is shown in Fig. 2g–k. In young flowers, *UGD2::GUS* activity can only be detected in the pistil. At later development stages, sepals and petals also show reporter gene activity (Fig. 2g). Also, *UGD2::GUS* activity is found in staminiferous and mature pollen (Fig. 2h). Siliques show *UGD2::GUS* activity in the abscission zone at the base and close to the top (Fig. 2k). No *UGD2::GUS* activity was observed in developing embryos or seeds.

In general, the expression patterns of *UGD2*, *3*, and *4* are very similar. However, *UGD1* shows an expression pattern which is distinct from that of the other isoforms. A comparison of the activity of the different *UGD* reporter gene constructs is shown in Fig. 3. In seedlings up to 4 d post-germination, *UGD2*, *3*, and *4::GUS* activity can only be detected in roots (Fig. 3a). This is in contrast to an almost inverse organ-specific pattern seen for *UGD1::GUS* (Fig, 3a). At 5 d post-germination this effect disappears. Furthermore, in young leaves, *UGD1* and *UGD4::GUS* show a cell type-specific activity in guard cells and in basal cells surrounding each trichome (Fig. 3e, f). All isoforms exhibit reporter gene activity in 3–4-week-old leaves at a low level, and differences in the activity pattern become visible again in the reproductive phase. Activity of all *UGD::GUS* reporter genes is seen in the stigma, the filaments, and the mature pollen (Fig. 3b, c). However, the activity of *UGD1::GUS* is limited to these tissues. *UGD3* and *4::GUS* reporter are also active in the flower bases. Only *UGD2::GUS* shows a strong activity in sepals and petals, and in pollen sacks (Fig. 3b, c). In developing siliques, the vascular system shows *UGD1*, *2*, and *3::GUS* activity (Fig. 3e, f), and *UGD2*, *3*, and *4::GUS* are strongly expressed in the abscission zone at the base of siliques (Fig. 3d).

Further analyses of expression of *UGD* genes in *Arabidopsis* via real-time PCR indicate that *UGD2* is usually expressed at the highest level of all *UGD* genes in seedlings (Fig. 4, upper panel). In roots of seedlings, *UGD2* and *3* are expressed at a very similar high level, while *UGD4* is expressed only weakly and no *UGD1* transcripts can be detected. Furthermore, in cotyledons and hypocotyl, *UGD2* expression dominates again, in addition to lower levels of *UGD3*. Publicly available microarray data from AtGenexpress were also analysed. The RNA for the microarray hybridization was from 7-d-old hypocotyls and 17-d-old roots. The relative transcript amounts for each

UGD gene are similar to our own data shown in the upper panel (Fig. 4, lower panel). As seen before with the reporter gene constructs, *UGD1* expression can be demonstrated in cotyledons and hypocotyl. In etiolated seedlings, *UGD2* and *UGD3* are predominantly expressed.

Expression of recombinant UGD in E. coli

UGD converts UDP-Glc into UDP-GlcA and is located at a critical partitioning step for carbohydrates between the storage compound sucrose via the enzyme SPS and building blocks for matrix polysaccharides via the enzyme UGD. To obtain a deeper insight into the biochemical properties of the different UGD isoforms, the individual enzymes were expressed as recombinant proteins in *E. coli* by cloning the ORF of each UGD isoform into a His-tag expression vector. Though UGDs from different sources have been investigated as recombinant proteins, it was found to be necessary to optimize thoroughly the expression conditions for each of the highly homologous isoforms. Modifications of the procedure for soybean UGD expression in *E. coli* (Hinterberg *et al.*, 2002) produced an adequate amount of active UGD2, 3, and 4 enzymes. An SDS–PAGE of the purified recombinant proteins, used for enzymatic analysis, is shown in Fig. 5. Several preparations of the recombinant proteins were analysed, which gave very similar data for the enzymatic activity. Expression of UGD1 could be obtained in *E. coli* but results in an inactive enzyme (data not shown). Several variations in *E. coli* culturing and protein purification conditions did not result in active recombinant UGD1 enzyme. Very recently Oka and Jigami (2006) published the expression of recombinant *Arabidopsis* UGD1 in yeast.

Enzyme kinetics

The affinity of the UGD isoforms for the cofactor NAD^+ does not differ between UGD2, 3, and 4. All enzymes exhibit typical hyperbolic reaction kinetics, with a K_m for NAD^+ of ~40–45 μM (Table 2). The high affinity of the enzyme for NAD^+ suggests that UGDs are not limited by the NAD^+ supply under physiological conditions.

In contrast to almost identical K_m values for NAD^+, the kinetic constants for UDP-Glc are highly dissimilar. UGD2 shows the highest affinity (of the UGDs studied here) for the substrate UDP-Glc, with a K_m of 123 μM, followed by UGD4 (171 μM) and UGD3 (335 μM) (Table 2). The catalytic constant k_{cat} was determined for the different isoforms with a value between 1.17 s^{-1} (UGD4) and 2.52 s^{-1} (UGD3) (see Table 2). Thus the different isoforms differ in the turnover rate of UDP-GlcA formation.

In some bacteria the activity of UGDs is modulated by phosphorylation on Tyr10, a conserved residue within the NAD-binding site (Mijakovic *et al.*, 2004). Recombinant UGDs were incubated with alkaline phosphatase, which can dephosphorylate the bacterial UGD (Mijakovic *et al.*,
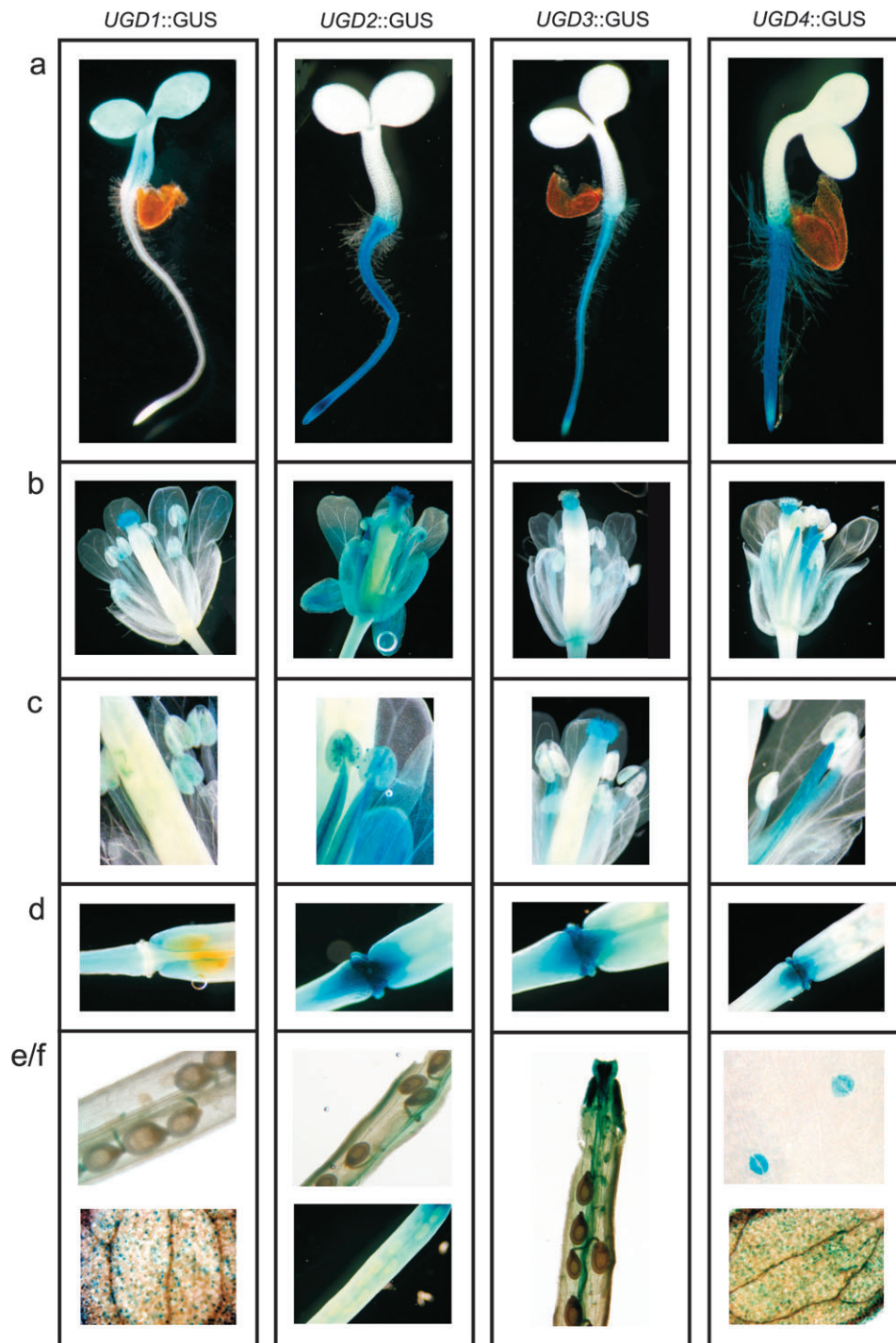
Fig. 3. *UGD::GUS* reporter gene expression in transgenic *Arabidopsis thaliana* plants reveals differential expression patterns for each UGD isoform (*UGD1–4*). (a) Two-day-old seedlings; (b) older flowers; (c) pollen sacs containing mature pollen; (d) base of siliques; (e, f) inside of siliques (manually opened; *UGD1, 2, 3::GUS* plants) and cotyledons with stained stomata (*UGD1, 4::GUS* plants).

2003, 2004), but no difference in the enzyme activity was found.

Fine tuning of UGD activity was reported to be mediated by feedback inhibition of the enzyme by UDP-xylose, a product obtained from UDP-GlcA after decarboxylation by the enzyme UDP-xylose synthase
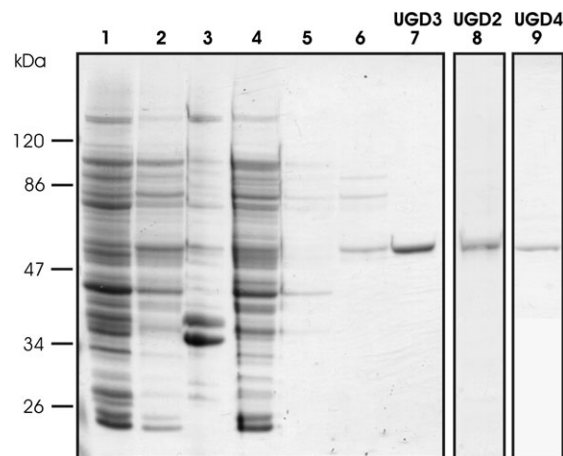
(Neufeld and Hall, 1965; Hinterberg *et al.*, 2002). The K_i value for UDP-xylose was determined for each isoform in the presence of different concentrations of UDP-Glc. The inhibition is competitive to UDP-Glc and therefore is seen mostly at low concentrations of UDP-Glc in the assays. UGD2 is more sensitively inhibited by UDP-xylose
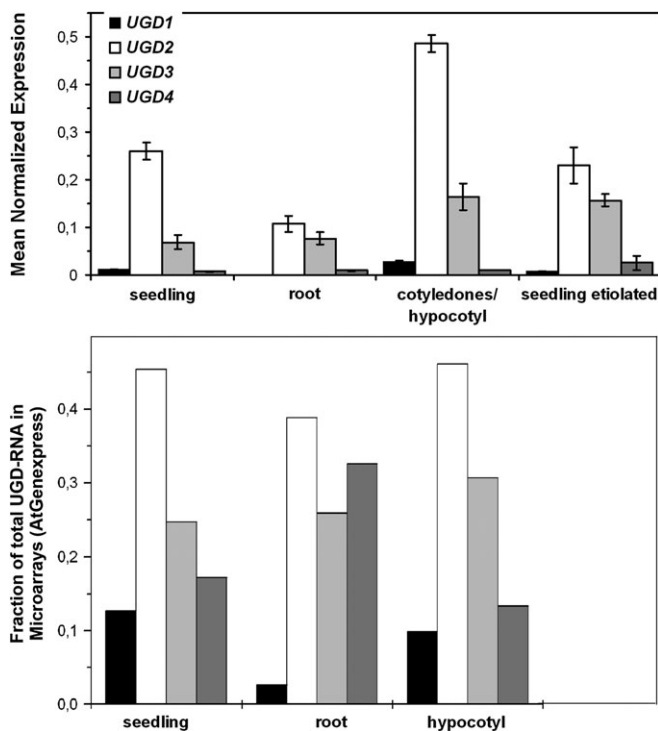
Fig. 4. Quantitative expression analysis (real-time PCR) of *UGD* transcripts in 6-d-old seedlings of *Arabidosis thaliana*. Upper panel: seedlings were grown under two conditions (light or dark) on half-strength MS medium with 0.5% sucrose. Data are presented as relative expression values normalized to the average of ubiquitin-5 mRNA, which was set to 1. Values represent the mean ±SD of three measurements. Lower panel: data from AtGenexpress microarrays were analysed for UGD expression. The sum of all UGD transcripts was set as 1 and the fraction for each isoform is shown in the bars. RNA from 7-d-old hypocotyls and 17-d-old roots was used in the experiments.

Fig. 5. SDS–PAGE analysis of recombinant UGD. Open reading frames of UGD2–4 were cloned into His-tagged expression vectors and transformed into *E. coli*. (a) Enzyme purification of active UGD3 (lanes 1–7) on SDS–PAGE (for purification details, see Materials and methods). Crude *E. coli* extract before IPTG induction (1) or 20 h after IPTG induction (2); (3) cell debris after centrifugation of disrupted *E. coli* cells; (4) column flow through; (5) flow through of washing step one; (6) flow through of washing step two; (7) purified recombinant UGD3 enzyme; lanes (8) and (9) show purification products of recombinant UGD2 and UGD3 enzyme; purification steps were carried out accordingly.

Table 2. *Kinetic analysis of UGD2, 3, and 4 from* Arabidopsis thaliana

Kinetic parameters were determined for the substrates UDP-glucose and NAD^+. Enzyme activity was measured as conversion of NAD^+ to NADH detected by the absorbance at 340 nm. Purified recombinant enzyme was incubated for 1 min with increasing concentrations of UDP-glucose (0.01–1.5 mM) in the presence of saturating NAD^+ (500 μM) or with increasing concentrations of NAD^+ (0.01–1.5 mM) in the presence of saturating UDP-glucose (1500 μM). Values represent the mean ±SD of three measurements.

| Isoform	K_m UDP-Glc (μM)	K_m NAD^+ (μM)	k_{cat} (s^{-1})
UGD2	123±9	43±6	1.92
UGD3	335±16	42±7	2.52
UGD4	171±9	44±7	1.17

(K_i ~83 μM) compared with UGD3 and 4, which exhibit a K_i of ~160 μM and 220 μM, respectively (Fig. 6a–c).

The superfamily of nucleotide-sugar dehydrogenases is quite conserved, and the substrate specificity cannot readily be predicted by bioinformatic tools. Therefore, different nucleotide-sugars were tested to determine if they are accepted as substrates for UGDs from *Arabidopsis* (Table 3). Unlike UDP, activated forms of glucose (ADP-Glc and TDP-Glc) are not converted into the corresponding NDP-GlcA derivatives, suggesting no direct interference with the starch biosynthesis pathway. In contrast to previous studies (Stewart and Copeland, 1998), no evidence for a direct oxidation of UDP-galactose into UDP-galacturonic acid was found. Products of the enzyme assay were separated by HPLC (Fig. 7). A time-dependent increase of the product UDP-GlcA was observed, directly correlating to the increase in NADH in the spectophotometric assay. The product analysis for the substrate specificity assays is shown in Fig. 7 using recombinant UGD1. This isoform has the highest number of amino acid changes from the UGD consensus sequences (compare Fig. 1) and was thus considered to be the most likely candidate for a

nucleotide-sugar dehydrogenase accepting substrates other than UDP-Glc. None of the four UGDs from *Arabidopsis* accepted UDP-galactose as a substrate (Fig. 7). In bacteria, members of the NDP-sugar dehydrogenase family use nucleotide-sugars such as GDP-mannose, UDP-galactose, UDP-*N*-acetylglucosamine or UDP-*N*-acetylgalactosamine as substrates. None of these potential substrates is accepted by the *Arabidopsis* UGDs. In summary, the data indicate that *Arabidopsis* has only true UGDs which accept UDP-Glc as their only substrate. The UGDs clearly prefer NAD^+ as a cofactor. Exchanging NAD^+ for $NADP^+$ greatly reduces the enzyme activity to ~20% (Table 3).

Discussion

The cell wall of *Arabidopsis* contains large amounts of hemi-celluloses and pectic polymers, which are predominantly
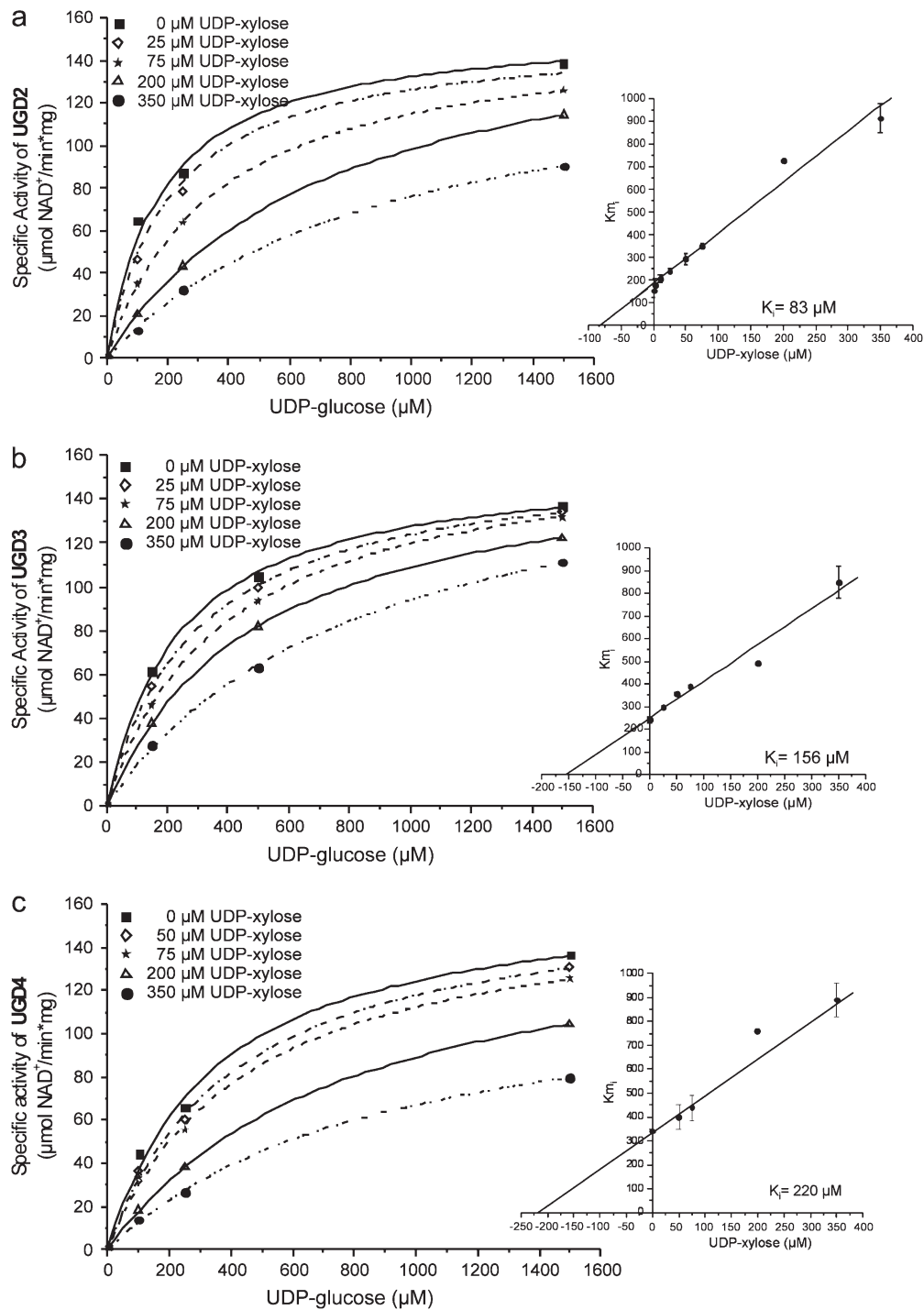
Fig. 6. Inhibitory effect of UDP-xylose on UGD2, 3, and 4 from *Arabidopsis thaliana*. Saturation curves of UDP-glucose at various inhibitor concentrations (25–350 μM) are shown. Additional plots represent the apparent K_m at different inhibitor concentrations revealing the K_i value. (a) UGD2; (b) UGD3; (c) UGD4.

derived from the common precursor UDP-GlcA (Zablackis *et al*., 1995). Therefore, biochemical pathways for the formation of UDP-GlcA are of great importance for the supply of glycosyl donors for polymer synthases and glycosyl transferases in the Golgi apparatus. As the nucleotide-sugars derived from UDP-GlcA are almost ex-

clusively used for the synthesis of cell wall material, the entry point of nucleotide-sugars into a pool for cell wall synthesis is tightly controlled. Previous studies have shown a close correlation between UGD transcripts and enzyme activity in *Arabidopsis* (Seitz *et al*., 2000). Furthermore, Gahan *et al*. (1997) and Johansson *et al*. (2002) have

Table 3. *Substrate specifity of UGD1, 2, 3. and 4 from* Arabidopsis thaliana

In standard enzyme assays either UDP-glucose or NAD$^+$ was substituted by alternative substrates. All nucleotide-sugars and cofactors were at a concentration of 1 mM. The detection limit is ~2–3% of the control.

| Nucleotide-sugar	Cofactor	Enzyme activity of isoforms (% of control)			
		UGD1	UGD2	UGD3	UGD4
UDP-glucose	NAD$^+$	100%	100%	100%	100%
UDP-glucose	NADP$^+$	Not tested	20%	20%	23%
ADP-glucose	NAD$^+$	n.d.[a]	n.d.	n.d.	n.d.
TDP-glucose	NAD$^+$	n.d.	n.d.	n.d.	n.d.
UDP-galactose	NAD$^+$	n.d.	n.d.	n.d.	n.d.
GDP-mannose	NAD$^+$	n.d.	n.d.	n.d.	n.d.
UDP-*N*-acetylglucosamine	NAD$^+$	n.d.	n.d.	n.d.	n.d.
UDP-*N*-acetylgalactosamine	NAD$^+$	n.d.	n.d.	n.d.	n.d

[a]n.d., not detected.

regarded UGD as a marker enzyme for developing xylem cells from cambium meristems in trees, because of a tight correlation between cell division, growth, and UGD enzyme activity. These studies have been extended by analysing the whole gene family of *UGD* genes from *Arabidopsis*. The available sequence data from the genome project as well as the sequenced EST libraries suggest four highly similar members of the *UGD* gene family in *Arabidopsis* (*UGD1–4*) in addition to a pseudogene (partial sequence). In the rice genome, at least five sequences for putative *UGD* genes can be identified (compare the tree in Fig. 1C). The presence of isoforms for UGDs was ignored in previous studies (Tenhaken and Thulke, 1996; Stewart and Copeland, 1998; Seitz *et al*., 2000; Turner and Botha, 2002). The main reason seems to be highly conserved amino acid sequences, which result in proteins with similar chromatographic properties.

Nucleotide-sugar dehydrogenases represent a large family of quite well conserved proteins, which oxidize the primary alcohol group at C6 of various sugars into the corresponding uronic acid (Roychoudhury *et al*., 1989). In bacteria, diverse substrates are converted by different family members. Based on multiple protein sequence alignments, it is likely that some of the annotations regarding the substrates are falsely assigned (data not shown). The PFAM database (http://www.sanger.ac.uk/Software/Pfam/) for patterns in proteins annotated the UGD-like genes from *Arabidopsis* and rice, and also plant EST sequences as 'UDP-glucose/GDP-mannose dehydrogenase family' (PF03721). This suggests that the substrate specificity of enzymes from this family cannot be predicted accurately by bioinformatics but needs experimental support. By expressing the proteins UGD1, 2, 3, and 4 as recombinant proteins, it has been shown here that they are true UGDs.

In the light of the separate nucleotide-sugar pools for cell wall synthesis and for sucrose synthesis, it is important to know whether UDP-Glc is the only entry point of nucleotide-sugars into the cell wall pool. Previously

Stewart and Copeland (1998) reported that one of the soybean UGDs also accepts UDP-galactose as a substrate, suggesting that the pectin precursor UDP-galacturonic acid may be directly derived from UDP-galactose. This possibility is excluded for the *Arabidopsis* UGDs based on the enzyme activity measurements with different potential substrates, which clearly indicate UDP-Glc as the only convertible substrate. As the measurement for UDP-Glc dehydrogenase activity in the study of Stewart and Copeland (1998) was based on an increase of NADH in the assay without analysis of the product, it seems possible either that the substrate UDP-galactose contained some residual UDP-Glc or that the enzyme preparation was contaminated with residual UDP-glucose-4-epimerase, which could have converted part of the UDP-galactose into UDP-Glc. The recent cloning of the genes encoding UDP-GlcA-4-epimerase (Mølhøj *et al*., 2004; Usadel *et al*., 2004), which produces UDP-galacturonic acid as glycosyl donor for pectic polymers, further supports this conclusion. Stewart and Copeland (1998) have purified a UDP-Glc dehydrogenase from soybean nodules, but the presence of isoforms was not considered. To our knowledge, only a single UGD from soybean has been characterized biochemically in more detail (Hinterberg *et al*., 2002), but evidence for the conversion of UDP-galactose was also not found in this study.

The biochemical data for the UGD isoforms from *Arabidopsis* showing a graded affinity for UDP-Glc and substrate turnover numbers suggest a role in the regulation of carbon fluxes into nucleotide-sugar pools for cell walls. During most of the life cycle of *Arabidopsis*, UGD2, 3, and 4 are co-expressed in the same tissues and thus different affinities for UDP-Glc and substrate turnover numbers might limit the use of too much UDP-Glc for cell wall polymers. In contrast, UGD1 has a high affinity for UDP-Glc (Oka and Jigami, 2006) but is expressed at low levels. Seitz *et al*. (2000) demonstrated a histochemical UGD activity stain in whole seedlings, which shows only
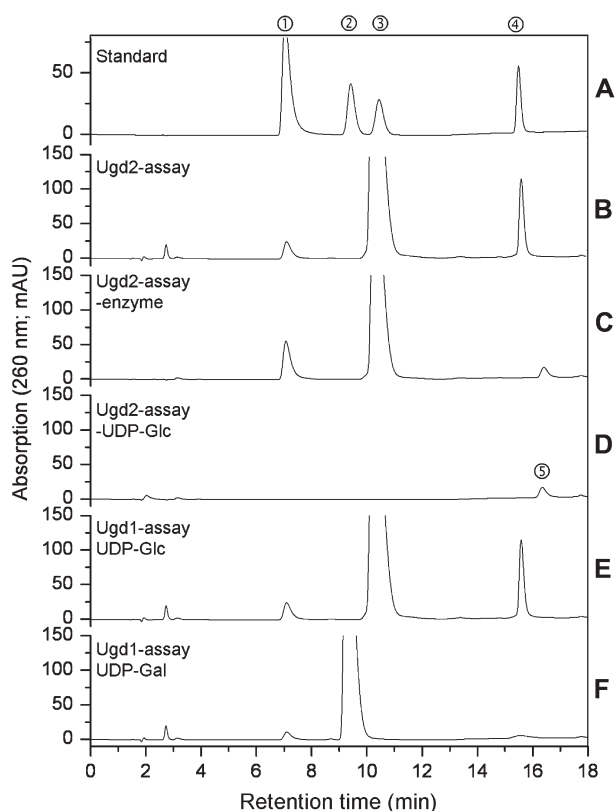
Fig. 7. Product analysis of UGD enzyme assays. (A) Standard compounds relevant for the enzyme assay (1, UMP; 2, UDP-Gal; 3, UDP-Glc; 4, UDP-GlcA). (B) UGD assay with recombinant UGD2, in which the substrate UDP-Glc is converted into UDP-GlcA. The minor peak in trace B corresponding to compound 1 represents UMP, a breakdown product of UDP-Glc hydrolysis. (C) Control assay in which the enzyme UGD2 was omitted. No UDP-GlcA product is formed. (D) Control assay in which UDP-Glc was omitted. The small peak #5 contains an unknown impurity. (E) Enzyme assays with recombinant UGD1 and substrate UDP-Glc, which is converted to UDP-GlcA by UGD1. (F) Enzyme assay with recombinant UGD1 and substrate UDP-Gal. UDP-Gal is not converted to an oxidized product but remains unchanged in the assay, indicating that UDP-Gal is not a substrate of UGD1.

a minor UGD activity in the hypocotyl compared with the primary root. In these seedlings, UGD1 is the major expressed isoform (compare Fig. 3). Kinetic constants for UGDs from different organisms vary over a wide range. One of the soybean UGDs, which has previously been characterized, has a high affinity for UDP-Glc (K_m ~21 µM; Hinterberg *et al.* 2002) similar to a UGD from sugarcane (K_m ~19 µM; Turner and Botha, 2002), whereas UGDs from maize (K_m=380 µM and 950 µM) show much higher K_m values (Kärkönen *et al.* 2005). The *Arabidopsis* UGDs have an intermediate K_m for UDP-Glc, ranging from 123 µM to 335 µM. Oka and Jigami (2006) determined a high affinity K_m (15.3 µM) for UDP-Glc for UGD1 from *Arabidopsis*. The high affinity of UGDs for UDP-Glc is correlated with a strong feedback inhibition by UDP-xylose (~10 µM in soybean; 17 µM in sugarcane)

but with much higher K_i values for the *Arabidopsis* UGD2, 3, and 4 (K_i 80–220 µM) as indicated in Table 2. Interestingly, Oka and Jigami (2006) determined the K_i of UDP-xylose for UGD1 to be 4.9 µM. This particular isoform also has a high affinity for the substrate UDP-Glc (15.3 µM), suggesting a structural modification of the enzyme substrate-binding pocket which increases the affinity for both the substrate UDP-Glc and the inhibitor UDP-Xyl. The k_{cat} values indicate a similar substrate conversion rate by the different isoforms, ranging from 1.17 s^{-1} for the slowest enzyme UGD4 to 2.52 s^{-1} for the fastest enzyme UGD3, and intermediate values for UGD2. These turnover rates agree well with data for the UGD from *S. pyogenes* (k_{cat}=1.8 s^{-1}) (Ge *et al.*, 2004) and the enzyme purified from bovine liver (k_{cat}= 2.92 s^{-1}; calculated on the basis of 50 kDa per subunit) (Zalitis and Feingold, 1969). In contrast, Bar-Peled *et al.* (2004) reported a much lower value for the UGD from *Cryptococcus neoformans* (k_{cat}=0.27 s^{-1}). The 2-fold difference in the turnover number between the *Arabidopsis* isoforms may well be important. UGD3 has the lowest affinity for UDP-Glc but the highest turnover number, indicating that the flux of UDP-sugars into UDP-GlcA by UGD3 is significant under conditions of a non-limited supply of UDP-Glc. Though the exact concentration of UDP-Glc in *Arabidopsis* leaves is not known and probably depends on environmental conditions as well, it can be assumed to be in the range of 1 mM. Dancer *et al.* (1990) estimated 3–4 mM UDP-Glc for spinach leaves. Farré *et al.* (2001) calculated 0.83 mM for the UDP-Glc concentration in potato tubers. The main competitor enzyme of UGDs for the substrate UDP-Glc is SPS, utilizing UDP-Glc for the biosynthesis of sucrose. The K_m values of SPSs for UDP-Glc are usually slightly higher than the K_m of UGDs reported here (Avigad, 1982). In addition, cellulose is synthesized from UDP-Glc or sucrose cleaved via membrane-bound isoforms of sucrose synthase into UDP-Glc and fructose. For example, cotton antisense plants for sucrose synthase have impaired cellulose trichomes, indicating an essential role for sucrose synthase in providing UDP-Glc for cellulose biosynthesis (Ruan *et al.*, 2003). The same mechanism may also apply to other β-glucan synthases (Buckeridge *et al.*, 1999; Konishi *et al.*, 2004). These findings suggest a supply of UDP-Glc from sucrose for various β-glucan synthases, which is presumably independent of the soluble UDP-Glc pool. Whether UGD uses UDP-Glc from cleaved sucrose to a larger extent is not known. However, strong evidence for this use is lacking, as indicated by the analysis of single and double knockout mutants in sucrose synthase, which show no cell wall mutant phenotypes (Bieniawska *et al.*, 2007). The flux of UDP-Glc into either sucrose or UDP-GlcA (for cell wall hemicelluloses) will therefore depend on several factors including the K_m for UDP-Glc of the enzymes, enzyme substrate turnover numbers, amount of enzyme, and post-translational

regulation of activity. In a recent paper by Park *et al.* (2007) the authors report on transgenic tobacco plants overexpressing an SPS gene, which have a reduced amount of arabinose and xylose in their cell wall. This indicates that the flux of UDP-Glc into hemicellulose material via UGD was displaced by favouring sucrose formation. Taking the data from reporter gene expression, real-time PCR, and knockout mutants (R Reboul, M Klinghammer, T Tenhaken, unpublished data), into account, it is concluded that UGD2 and UGD3 are the major contributing enzymes for the flux from UDP-Glc into UDP-GlcA in *Arabidopsis*.

Acknowledgements

References

Amrein KE, Takacs B, Stieger M, Molnos J, Flint NA, Burn P. 1995. Purification and characterization of recombinant human p50csk protein-tyrosine kinase from an *Escherichia coli* expression system overproducing the bacterial chaperones GroES and GroEL. *Proceedings of the National Academy of Sciences, USA* **92,** 1048–1052.

Avigad G. 1982. Sucrose and other disaccharides. In: Loewus FA, Tanner W, eds. *Encyclopedia of plant physiology*. Berlin: Springer-Verlag, 217–347.

Bar-Peled M, Griffith CL, Ory JJ, Doering TL. 2004. Biosynthesis of UDP-GlcA, a key metabolite for capsular polysaccharide synthesis in the pathogenic fungus *Cryptococcus neoformans*. *Biochemical Journal* **381,** 131–136.

Bieniawska Z, Paul Barratt DH, Garlick AP, Thole V, Kruger NJ, Martin C, Zrenner R, Smith AM. 2007. Analysis of the sucrose synthase gene family in Arabidopsis. *The Plant Journal* **49,** 810–828.

Buckeridge MS, Vergara CE, Carpita NC. 1999. The mechanism of synthesis of a mixed-linkage $(1\rightarrow 3)$, $(1\rightarrow 4)$beta-D-glucan in maize. Evidence for multiple sites of glucosyl transfer in the synthase complex. *Plant Physiology* **120,** 1105–1116.

Burget EG, Verma R, Molhoj M, Reiter WD. 2003. The biosynthesis of L-arabinose in plants: molecular cloning and characterization of a Golgi-localized UDP-D-xylose 4-epimerase encoded by the MUR4 gene of Arabidopsis. *The Plant Cell* **15,** 523–531.

Campbell RE, Mosimann SC, van De Rijn I, Tanner ME, Strynadka NC. 2000. The first structure of UDP-glucose dehydrogenase reveals the catalytic residues necessary for the two-fold oxidation. *Biochemistry* **39,** 7012–7023.

Chomczynski P, Sacchi N. 1987. Single step method of RNA isolation by acid guanidinium thiocyanate–phenol–chloroform extraction. *Analytical Biochemistry* **162,** 156–159.

Clough SJ, Bent AF. 1998. Floral dip: a simplified method for *Agrobacterium*-mediated transformation of *Arabidopsis thaliana*. *The Plant Journal* **16,** 735–743.

Dancer J, Neuhaus HE, Stitt M. 1990. Subcellular compartmentation of uridine nucleotides and nucleoside-5′-diphosphate kinase in leaves. *Plant Physiology* **92,** 637–641.

Farré EM, Tiessen A, Roessner U, Geigenberger P, Trethewey RN, Willmitzer L. 2001. Analysis of the compartmentation of glycolytic intermediates, nucleotides, sugars, organic acids, amino acids, and sugar alcohols in potato tubers using a non-aqueous fractionation method. *Plant Physiology* **127,** 685–700.

Gahan PB, McGarry A, Wang L, Doré T, Carmignac DF. 1997. Glucose-6-phosphate and UDP-D-glucose dehydrogenases: possible markers of vascular differentiation. *Phytochemical Analysis* **8,** 110–114.

Ge X, Penney LC, van de Rijn I, Tanner ME. 2004. Active site residues and mechanism of UDP-glucose dehydrogenase. *European Journal of Biochemistry* **271,** 14–22.

Gibeaut DM. 2000. Nucleotide sugars and glycosyltransferases for synthesis of cell wall matrix polysaccharides. *Plant Physiology and Biochemistry* **38,** 69–80.

Hinterberg B, Klos C, Tenhaken R. 2002. Functional characterization of recombinant UDP-glucose dehydrogenase from soybean. *Plant Physiology and Biochemistry* **40,** 1011–1017.

Jefferson RA. 1987. Assaying chimeric genes in plants: the GUS gene fusion system. *Plant Molecular Biology Reports* **5,** 387–405.

Johansson H, Sterky F, Amini B, Lundeberg J, Klexzkowsli LA. 2002. Molecular cloning and characterization of a cDNA encoding poplar UDP-glucose dehydrogenase, a key gene of hemicellulose/pectin formation. *Biochimica et Biophysica Acta* **1576,** 53–58.

Kanter U, Usadel B, Guerineau F, Li Y, Pauly M, Tenhaken R. 2005. The inositol oxygenase gene family of Arabidopsis is involved in the biosynthesis of nucleotide sugar precursors for cell-wall matrix polysaccharides. *Planta* **221,** 243–254.

Kärkönen A, Murigneux A, Martinant JP, Pepey E, Tatout C, Dudley BJ, Fry SC. 2005. UDP-glucose dehydrogenases of maize: a role in cell wall pentose biosynthesis. *Biochemical Journal* **391,** 409–415.

Karsai A, Muller S, Platz S, Hauser MT. 2002. Evaluation of a home-made SYBR green I reaction mixture for real-time PCR quantification of gene expression. *Biotechniques* **32,** 790–796.

Kobayashi M, Nakagawa H, Suda I, Miyagawa I, Matoh T. 2002. Purification and cDNA cloning of UDP-D-glucuronate carboxy-lyase (UDP-D-xylose synthase) from pea seedlings. *Plant and Cell Physiology* **43,** 1259–1265.

Konishi T, Ohmiya Y, Hayashi T. 2004. Evidence that sucrose loaded into the phloem of a poplar leaf is used directly by sucrose synthase associated with various beta-glucan synthases in the stem. *Plant Physiology* **134,** 1146–1152.

Loewus FA, Kelly S, Neufeld EF. 1962. Metabolism of myo-inositol in plants: conversion to pectin, hemicellulose, D-xylose and sugar acids. *Proceedings of the National Academy of Sciences, USA* **48,** 421–425.

Mijakovic I, Petranovic D, Deutscher J. 2004. How tyrosine phosphorylation affects the UDP-glucose dehydrogenase activity of *Bacillus subtilis* YwqF. *Journal of Molecular Microbiology and Biotechnology* **8,** 19–25.

Mijakovic I, Poncet S, Boel G, et al. 2003. Transmembrane modulator-dependent bacterial tyrosine kinase activates UDP-glucose dehydrogenases. *EMBO Journal* **22,** 4709–4718.

Mølhøj M, Verma R, Reiter WD. 2004. The biosynthesis of D-galacturonate in plants. Functional cloning and characterization of a membrane-anchored UDP-D-glucuronate-4-epimerase from Arabidopsis. *Plant Physiology* **135,** 1221–1230.

Neufeld EF, Hall CW. 1965. Inhibition of UDP-D-glucose dehydrogenase by UDP-D-xylose: a possible regulatory mechanism. *Biochemical and Biophysical Research Communications* **19,** 456–461.

Oka T, Jigami Y. 2006. Reconstruction of de novo pathway for synthesis of UDP-glucuronic acid and UDP-xylose from intrinsic UDP-glucose in *Saccharomyces cerevisiae*. *FEBS Journal* **273,** 2645–2657.

Park JY, Canam T, Kang KY, Ellis DD, Mansfield SD. 2007. Over-expression of an Arabidopsis synthase (SPS) gene alters plant growth and fibre development. *Transgenic Research* (in press) DOI 10.1007/s11248-007-9090-2.

Reiter W, Vanzin GF. 2001. Molecular genetics of nucleotide sugar interconversion pathways in plants. *Plant Molecular Biology* **47,** 95–113.

Roychoudhury S, May TB, Gill JF, Singh SK, Feingold DS, Chakrabarty AM. 1989. Purification and characterization of guanosine diphospho-D-mannose dehydrogenase. A key enzyme in the biosynthesis of alginate by *Pseudomonas aeruginosa*. *Journal of Biological Chemistry* **264,** 9380–9385.

Ruan YL, Llewellyn DJ, Furbank RT. 2003. Suppression of sucrose synthase gene expression represses cotton fiber cell initiation, elongation, and seed development. *The Plant Cell* **15,** 952–964.

Seifert GJ. 2004. Nuceleotide sugar interconversions and cell wall biosynthesis: how to bring the inside to the outside. *Current Opinion in Plant Biology* **7,** 277–284.

Seitz B, Klos C, Wurm M, Tenhaken R. 2000. Matrix polysaccharide precursors in Arabidopsis cell walls are synthesised by alternative pathways with organ specific expression patterns. *The Plant Journal* **21,** 537–546.

Stewart DC, Copeland L. 1998. Uridine-5′-diphosphate dehydrogenase from soybean nodules. *Plant Physiology* **116,** 349–355.

Tenhaken R, Thulke O. 1996. Cloning of an enzyme that synthesizes a key nucleotide sugar precursor of hemicellulose biosynthesis from soybean: UDP-glucose dehydrogenase. *Plant Physiology* **112,** 1127–1134.

Turner W, Botha FC. 2002. Purification and kinetic properties of UDP-glucose dehydrogenase from sugarcane. *Archives of Biochemistry and Biophysics* **407,** 209–216.

Usadel B, Schluter U, Mølhøj M, Gipmans M, Verma R, Kossmann J, Reiter WD, Pauly M. 2004. Identification and characterization of a UDP-D-glucuronate 4-epimerase in Arabidopsis. *FEBS Letters* **569,** 327–331.

Winter H, Huber SC. 2000. Regulation of sucrose metabolism in higher plants: localization and regulation of activity of key enzymes. *Critical Reviews in Biochemistry and Molecular Biology* **35,** 253–289.

Zablackis E, Huang J, Muller B, Darvill AG, Albersheim P. 1995. Characterization of the cell-wall polysaccharides of *Arabidopsis thaliana* leaves. *Plant Physiology* **107,** 1129–1138.

Zalitis J, Feingold DS. 1969. Purification and properties of UDPG dehydrogenase from beef liver. *Archives of Biochemistry and Biophysics* **132,** 457–465.